

See discussions, stats, and author profiles for this publication at: <https://www.researchgate.net/publication/232819297>

# Genetic-Algorithm-Based Computational Models for Optimizing the Process Parameters of A-TIG Welding to Achieve Target Bead Geometry in Type 304 L(N) and 316 L(N) Stainless Steels

Article in *Materials and Manufacturing Processes* · June 2007

DOI: 10.1080/10426910701323342

CITATIONS

60

READS

2,103

4 authors, including:



**M. Vasudevan**

Indira Gandhi Centre for Atomic Research

195 PUBLICATIONS 3,351 CITATIONS

SEE PROFILE



**Baldev Raj**

Indira Gandhi Centre for Atomic Research

919 PUBLICATIONS 18,386 CITATIONS

SEE PROFILE



**Prasad Kalvala**

University of Utah

165 PUBLICATIONS 5,845 CITATIONS

SEE PROFILE

Some of the authors of this publication are also working on these related projects:



FEM and CFD of welding processes [View project](#)



Studies on Hampi Musical Pillars [View project](#)

This article was downloaded by:[Raj, Baldev]  
[Raj, Baldev]

On: 19 June 2007

Access Details: [subscription number 779151586]

Publisher: Taylor & Francis

Informa Ltd Registered in England and Wales Registered Number: 1072954

Registered office: Mortimer House, 37-41 Mortimer Street, London W1T 3JH, UK



## Materials and Manufacturing Processes

Publication details, including instructions for authors and subscription information:  
<http://www.informaworld.com/smpp/title~content=t713597284>

### Genetic-Algorithm-Based Computational Models for Optimizing the Process Parameters of A-TIG Welding to Achieve Target Bead Geometry in Type 304 L(N) and 316 L(N) Stainless Steels

To cite this Article: Vasudevan, M., Bhaduri, A. K., Raj, Baldev and Rao, K. Prasad , 'Genetic-Algorithm-Based Computational Models for Optimizing the Process Parameters of A-TIG Welding to Achieve Target Bead Geometry in Type 304 L(N) and 316 L(N) Stainless Steels', Materials and Manufacturing Processes, 22:5, 641 - 649

To link to this article: DOI: 10.1080/10426910701323342

URL: <http://dx.doi.org/10.1080/10426910701323342>

PLEASE SCROLL DOWN FOR ARTICLE

Full terms and conditions of use: <http://www.informaworld.com/terms-and-conditions-of-access.pdf>

This article maybe used for research, teaching and private study purposes. Any substantial or systematic reproduction, re-distribution, re-selling, loan or sub-licensing, systematic supply or distribution in any form to anyone is expressly forbidden.

The publisher does not give any warranty express or implied or make any representation that the contents will be complete or accurate or up to date. The accuracy of any instructions, formulae and drug doses should be independently verified with primary sources. The publisher shall not be liable for any loss, actions, claims, proceedings, demand or costs or damages whatsoever or howsoever caused arising directly or indirectly in connection with or arising out of the use of this material.

© Taylor and Francis 2007

# Genetic-Algorithm-Based Computational Models for Optimizing the Process Parameters of A-TIG Welding to Achieve Target Bead Geometry in Type 304 L(N) and 316 L(N) Stainless Steels

M. VASUDEVAN<sup>1</sup>, A. K. BHADURI<sup>1</sup>, BALDEV RAJ<sup>1</sup>, AND K. PRASAD RAO<sup>2</sup>

<sup>1</sup>Indira Gandhi Centre for Atomic Research, Kalpakkam, India

<sup>2</sup>Department of Metallurgical and Materials Engineering, Indian Institute of Technology Madras, Chennai, India

The weld-bead geometry in 304LN and 316LN stainless steels produced by A-TIG welding plays an important role in determining the mechanical properties of the weld and its quality. Its shape parameters such as bead width, depth of penetration, and reinforcement height are decided according to the A-TIG welding process parameters such as current, voltage, torch speed, and arc gap. Identification of a suitable combination of A-TIG process parameters to produce the desired weld-bead geometry required many experiments, and the experimental optimization of the A-TIG process was indeed time consuming and costly. Therefore it becomes necessary to develop a methodology for optimizing the A-TIG process parameters to achieve the target weld-bead geometry. In the present work, genetic algorithm (GA)-based computational models have been developed to determine the optimum/near optimum process parameters to achieve the target weld-bead geometry in 304LN and 316LN stainless steel welds produced by A-TIG welding.

*Keywords* A-TIG welding; Austenitic stainless steels; Genetic algorithm; Weld bead geometry.

## 1. INTRODUCTION

TIG welding is extensively used in the fabrication of the structural components of Fast Breeder Reactors. Tungsten inert gas (TIG) welding is generally used to produce single pass full penetration welds and root pass of multi-pass welds. The principal disadvantages of TIG welding lie in the limited thickness of material which can be welded in a single pass, poor tolerance to some material composition (cast-to-cast variations), and low productivity. Weld penetration achievable in single pass TIG welding of stainless steel is limited to 3 mm when using argon as shielding gas. This can be improved to 4–5 mm by using helium as shielding gas which, because of its higher ionization potential, produces a higher temperature arc. In addition, austenitic stainless steel exhibits variable weld joint penetration during TIG welding due to small differences in chemical composition between heats of material [1, 2]. Variable weld penetration has been observed when welding austenitic stainless steels especially in autogenous TIG welds or the root pass of multiple pass TIG welds. Poor productivity in TIG welding results from a combination of low welding speeds and in thicker material the high number of passes required to fill the joint. Over the years, several strategies have been adopted to improve penetration depth or productivity of the TIG process. Very high currents can be used in automated TIG processes to increase penetration, but defects may form, and the process becomes unstable above 500 A. The keyhole mode Gas Tungsten Arc Welding (GTAW) process which was developed a few years ago, seems to be suitable for thickness in the range 3–12 mm for both ferrous

and nonferrous materials [3]. However, this technique is sensitive to arc voltage and loss of material may occur through the keyhole vent.

A novel variant of the TIG welding process called the A-TIG is reported to enhance the penetration capability of TIG welding for joining thickness of 10–12 mm by single pass welding. In this process, the penetration capability of the arc in TIG welding can be significantly increased by applying flux coating containing certain inorganic compounds on the joint surface prior to welding [4–10]. There is interest in developing this process for various alloys. Figure 1 shows a visible constriction of the arc in A-TIG welding compared with the more diffuse conventional TIG arc at the same current level. The schematic sketch of the typical weld-bead profiles obtained in conventional TIG and A-TIG welding are compared in Fig. 2. The use of flux is supposed to reduce the susceptibility to changes in penetration caused by cast-to-cast variability in material composition and produce consistent penetration regardless of heat-to-heat variations in base metal compositions [8, 11]. In particular, research has focused on the A-TIG welding process developed by the E. O. Paton Electric Welding Institute (PWI) [5]. Limited published information regarding the use and composition of the flux attracted attention in the 1990s, including the researchers at the Edison Welding Institute (EWI) and The Welding Institute (TWI), U.K. In this process, the A-TIG flux in the form of paste (flux dissolved in acetone) is applied on the joint prior to welding by using a brush. The acetone is evaporated leaving flux on the surface, and autogenous TIG welding is carried out. It has been claimed that the A-TIG process can achieve, in a single pass, a full penetration weld in steels and stainless steels up to 12 mm thickness without using a bevel preparation or filler wire [11]. Furthermore the weldment mechanical properties and soundness are claimed to be unaffected.

Received July 21, 2006; Accepted November 15, 2006

Address correspondence to Baldev Raj, Indira Gandhi Centre for Atomic Research, Kalpakkam 603 102, India; E-mail: dev@igcar.gov.in

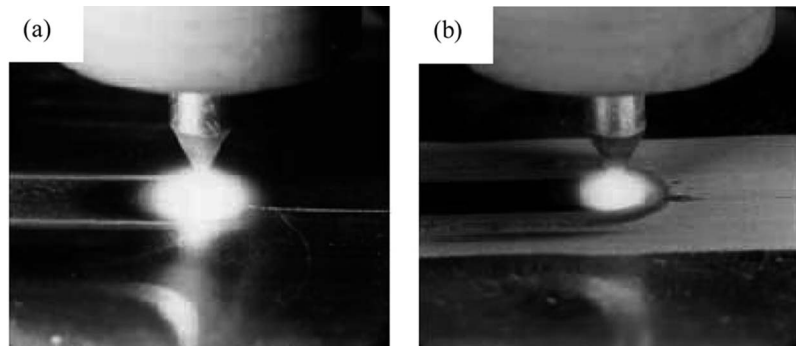


FIGURE 1.—Characteristic appearance of the TIG arc in argon shielding gas in (a) conventional TIG (b) A-TIG welding.

Activated flux for single pass TIG welding of 304 LN and 316 LN stainless steels up to 10–12 mm in thickness has been developed in our laboratory. In this process, to produce the desired depth of penetration or bead geometry, it is very important to select the right combination of process parameters. However this requires many experiments, and the experimental optimization of this process is very costly and time consuming. Therefore it becomes necessary to develop a convenient tool for optimizing the process parameters to achieve the target geometry in 304 LN and 316 LN stainless steels produced by A-TIG welding.

Genetic algorithms (GAs) are search algorithms based on the mechanics of natural selection and genetics. These methods are based on Darwin's theory of survival of the fittest and belong to the GA of stochastic search methods. A good introduction to GA can be found in Deb [12]. In GA, the initial population is the possible solution to the optimization problem and each possible solution is called an *individual*. Each individual is represented as a binary string consisting of combinations of randomly generated 0s and 1s [13]. Coding the parameter in a binary string is primarily used in order to have a pseudochromosomal representation of a solution [12]. They are very effective in exchanging information between each individual, and need to be changed into real numbers for evaluating the fitness. The fitness evaluation is a procedure necessary to decide the survival of each individual, with the individual with large fitness value representing better solutions. The next step is to use each individual's fitness and the genetic operators (reproduction, crossover, and mutation) to produce the next generation of population. Reproduction is the process in which each individual is duplicated according to its fitness, and the individual with higher fitness produces more offspring in the next generation than that with lower

fitness. This explains Darwin's survival-of-the-fittest theory. Crossover is the process by which the strings are able to mix and match their attributes through random process. Crossover proceeds in the following three steps:

- (1) Random selection of two parent strings from the mating pool;
- (2) Random selection of an arbitrary location in both strings;
- (3) Exchange of the portions of the strings following the crossover site between two parent strings to form two offspring strings.

This crossover does not occur with all strings, but is limited by the crossover rate. For example, if the crossover rate is 0.9, then crossover occurs in 90% of the pairs, whereas the remaining 10% are added to the next generation without crossover. After crossover, mutation is performed by occasionally altering the value of a string position. Each bit value in every string is a candidate for mutation and its selection is determined by the mutation rate. The mutation rate is usually set to a low value to avoid losing good strings. In GA, the population size, crossover rate, and mutation rate are important factors in the performance of the algorithm and have to be optimized.

GA modeling has been adapted for large number of applications in material processing ranging from iron and steel production [14, 15], continuous casting process [16], conventional casting process [17], metal forming process [18], and powder metallurgy process [19]. Recently, GA is increasingly being used for determining the optimum welding process variables to achieve the desired weld attributes. GA modeling has been used for determining the optimal/near-optimal settings of the Gas Metal Arc (GMA) welding process parameters to achieve the target geometry [20]. The output variables were the bead height and the depth of penetration of the weld bead. These output variables were determined according to the input variables which are the root opening, wire feed rate, welding voltage, and welding speed. The study demonstrated how to obtain near-optimal welding conditions over a wide search space, conducting a relatively small number of experiments. Using GA and response surface methodology, modeling and optimization of the GMA welding process has been studied in detail [21, 22]. In this study the dual response approach is adopted to determine the welding process parameters which produce the

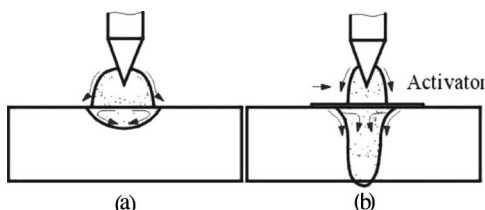


FIGURE 2.—Schematic sketch of penetration in (a) conventional TIG and (b) A-TIG welding.

target value with minimal variance. First regression models are generated. Subsequently, a GA based on the regression models and constraints is applied to determine the welding process parameters that generate the desired penetration with minimum variance. For optimizing the process parameters during welding of brass plates, Cemal Meran [23] has applied GA-based modes for estimating the current and velocity in order to minimize the evaporation of brass material. Good quality weld beads could be obtained by employing GA-based models.

Correia et al. [24] have also applied GA to decide the near-optimal settings of a GMA welding process. In their study, the search for near-optimal was carried out step by step with the GA predicting the next experiment based on the previous and without the knowledge of the modeling equations between the inputs and outputs of the GMA welding process. By using GA it was possible to locate near-optimum conditions with relatively few experiments. The bi-directional capability of the heat transfer and fluid-flow models is attained by coupling the heat-transfer and fluid-flow calculations with a GA [25, 26]. In addition, the capability to determine alternate paths to achieve a target geometry is demonstrated by estimating the various sets of current, voltage, welding speed, and wire feed rate that can all produce target weld geometry. Kumar and Debroy [26] demonstrated that the coupling of numerical heat and fluid-flow model with a GA to arrive at the optimum process parameters in order to achieve the target geometry in Gas Tungsten Arc (GTA) welding of low-alloy steel fillet welds. The study provided hope that weld attributes can be tailored reliably through multiple routes based on heat-transfer and fluid-flow calculations and evolutionary algorithms.

Therefore, GA modeling has been demonstrated to be an efficient method for nonlinear optimization of welding process parameters for various welding processes. The present work aims at developing GA-based computational models to determine the optimal/near-optimal A-TIG welding process parameters for achieving the target weld-bead geometry in 304 LN and 316 LN stainless steel welds produced by A-TIG welding.

## 2. EXPERIMENTAL

Bead-on-plate welds using a multicomponent flux were made on 304LN and 316LN stainless steel plates of 10 mm and 12 mm thickness, respectively, under varying process conditions. Table 1 gives the various process conditions used for making the bead-on-plate welds. Typical bead-on-plate A-TIG welds on 304LN and 316LN stainless

TABLE 1.—Process parameters for making bead-on-plate welds on 304LN and 316LN stainless steel using A-TIG process.

Welding parameter	Selection
Current	80, 100, 120, 140, 160, 180, 200, 220, 240, 280 A
Torch speed	1, 1.33, 1.67, 2, 2.67 and 3.33 mm/sec
Arc gap	0.75 and 1.5 mm
Shielding gas	Argon; flow rate =10 l/min
Electrode	Thoriated Tungsten, 3 mm dia.
Electrode tip angle	45°
Flux type	Multicomponent

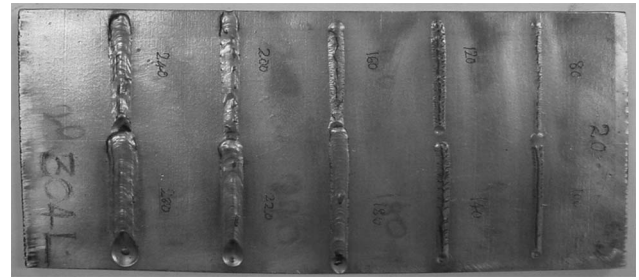


FIGURE 3.—Bead-on-plate A-TIG welds on 10 mm thick 304LN stainless steel plate.

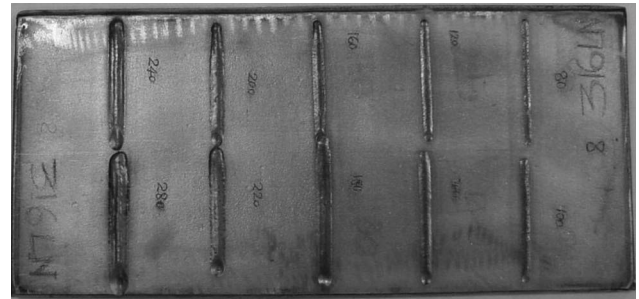


FIGURE 4.—Bead-on-plate A-TIG welds on 12 mm thick 316LN stainless steel plate.

steel plates are shown in Figs. 3 and 4, respectively. Samples cut from the welds were polished and etched to see the macrostructure. Measurements on weld-bead shape parameters such as depth of penetration, weld-bead width, and reinforcement height were carried out using a microscope. The data generated based on these experiments were used to generate regression models correlating the weld-bead shape parameters with welding process parameters using multiple regression.

## 3. RESULTS AND DISCUSSION

The development of methodology for optimizing A-TIG welding process parameters using a GA was done in two steps. First, regression models were developed correlating the A-TIG welding process parameters with the three weld-bead shape parameters, viz. bead width (BW), depth of penetration (DOP), and reinforcement height (RH) using the generated data. Then a GA code was developed using MATLAB version 6.1 in which the objective function was evaluated using the regression models.

### 3.1. Development of Regression Models for 304LN Stainless Steel Welds Produced by A-TIG Welding

Regression models were developed using the data (120 nos) generated using a multiple regression method. The relationship between the three weld-bead shape parameters and the welding process variables obtained from the regression models, the corresponding regression coefficients and the standard errors of estimates are as follows. (Other terms such as  $V * S$ ,  $V * G$ ,  $S * G$ , and  $G * G$  are not

included in the regression equation as the coefficient values were found to be very insignificant):

$$\begin{aligned} \text{DOP} = & 0.27946 + 0.04961 * I + 0.11002 * V \\ & - 0.21162 * S - 0.53303 * G \\ & - 0.00141 * I * V \\ & - 0.0014 * I * S + 0.00316 * I * G \\ & + 0.0000437177 * I^2 + 0.01065 * S^2 \end{aligned} \quad (1)$$

Regression coefficient = 0.97;  
Standard deviation = 0.32

$$\begin{aligned} \text{RH} = & -0.30796 + 0.0004187 * I + 0.10023 * V \\ & - 0.01046 * S - 0.28719 * G \\ & - 0.0007915 * I * V \\ & + 0.00001245 * I * S + 0.00202 * I * G \\ & + 0.00003797 * I^2 + 0.00004965 * S^2 \end{aligned} \quad (2)$$

Regression coefficient = 0.75;  
Standard deviation = 0.10

$$\begin{aligned} \text{BW} = & 0.38168 + 0.0854 * I + 0.28924 * V \\ & - 0.1794 * S \\ & + 0.2496 * G - 0.0002042 * I * V \\ & - 0.0005326 * I * S + 0.0009386 * I * G \\ & + 0.00003310 * I^2 + 0.00664 * S^2 \end{aligned} \quad (3)$$

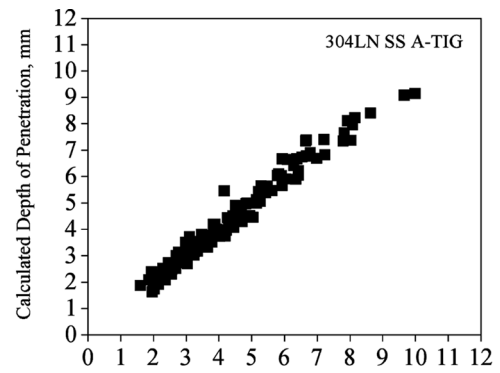
Regression coefficient = 0.96;  
Standard deviation = 0.42

Close agreement was obtained between the calculated and measured values of the three weld-bead shape parameters as shown in Figs. 5(a)–(c). Thus, all three regression models given in Eqs. (1)–(3) exhibit good correlation between the welding process variables and the weld-bead shape parameters.

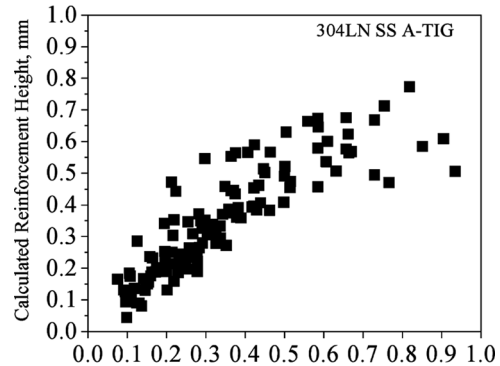
### 3.2. Development of Regression Models for 316LN Stainless Steel Welds Produced by A-TIG Welding

Regression models were developed using the data (120 nos) generated using the multiple regression method. The relationship between the three weld-bead shape parameters and the welding process variables obtained from the regression models, the corresponding regression coefficients, and the standard errors of estimates are as follows. (Other terms such as  $V * S$ ,  $V * G$ ,  $S * G$ , and  $G * G$  are not included in the regression equation as the coefficient values were found to be very insignificant.):

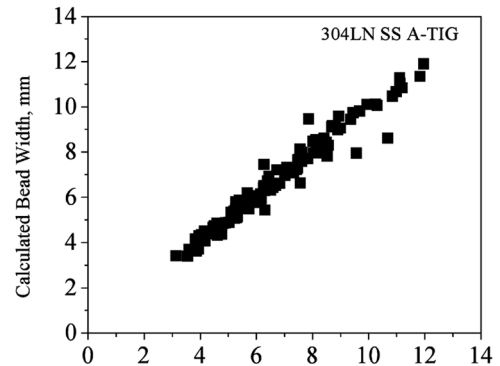
$$\begin{aligned} \text{DOP} = & 3.01558 + 0.0379 * I - 0.25428 * V \\ & - 0.1739 * S - 0.62295 * G + 0.00149 * I * V \\ & - 0.00165 * I * S + 0.00421 * I * G \end{aligned}$$



(a)



(b)



(c)

FIGURE 5.—Comparison between the measured and calculated weld-bead shape parameters (a) depth of penetration (b) reinforcement height (c) weld-bead width for 304LN stainless steel welds produced by A-TIG welding.

$$\begin{aligned} & - 0.00005315 * I^2 + 0.01092 * S^2 \end{aligned} \quad (4)$$

Regression coefficient = 0.98;  
Standard deviation = 0.30

$$\begin{aligned} \text{RH} = & 0.45532 + 0.00208 * I - 0.0482 * V \\ & - 0.02179 * S + 0.09639 * G \\ & + 0.00021488 * I * V \\ & - 0.00010541 * I * S - 0.00074437 * I * G \end{aligned}$$

$$+ 0.00000099065 * I^2 + 0.00107 * S^2 \quad (5)$$

Regression coefficient = 0.88;

Standard deviation = 0.08

$$BW = 0.74911 + 0.01676 * I + 0.27256 * V$$

$$- 0.01758 * S - 0.00438 * G + 0.0011 * I * V$$

$$- 0.000357638 * I * S + 0.0006766 * I * G$$

$$- 0.000052662 * I^2 - 0.00029521 * S^2 \quad (6)$$

Regression coefficient = 0.98;

Standard deviation = 0.29

Close agreement was obtained between the calculated and measured values of all three weld-bead shape parameters as shown in Figs. 6(a)–(c). Thus, all three regression models given in Eqs. (4)–(6) exhibit good correlation between the weld-bead shape parameters and the welding process variables.

### 3.3. Development of Code for GA

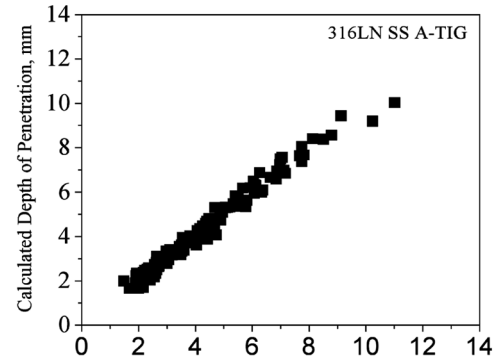
The code for the genetic algorithm was developed in MATLAB version 6.1 for optimizing the A-TIG process parameters for obtaining the target bead geometry during welding of 304LN and 316LN stainless steels. The flow chart describing the various steps involved in the execution of the GA is given in Fig. 7, in which the *Search Space* defines the range of the input parameters,  $I$ ,  $V$ ,  $S$ , and  $G$  (Table 1), within which the GA searches for optimal solution.

### 3.4. Development of the Objective Function

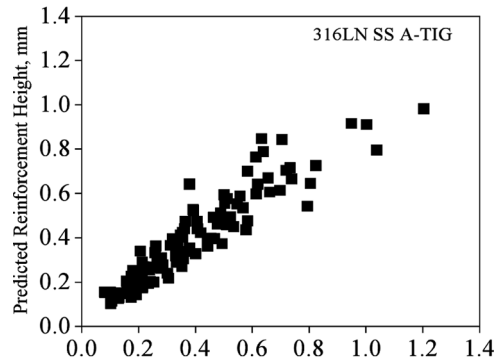
To achieve the target values of the three weld-bead shape parameters (DOP, BW, RH) in the weld-bead geometry, there can be more than one set of process variables. Hence, the objective function that is used should direct the solution to convergence. Generally, least-square error minimization is used as an objective function. In the present work, the sum of the least-square errors for the three weld-bead shape parameters was chosen as the objective function given below:

$$obj V = \left( \frac{RHT - RH(i)}{RHT} \right)^2 + \left( \frac{BW - BW(i)}{BW} \right)^2 + \left( \frac{DOP - DOP(i)}{DOP} \right)^2 \quad (7)$$

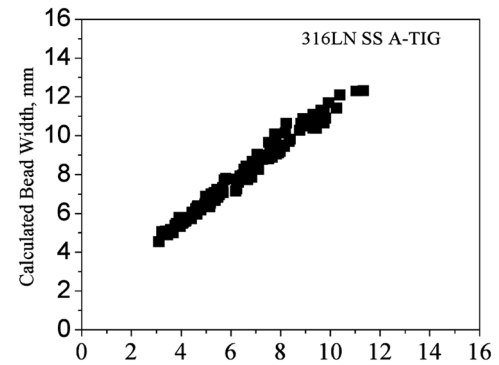
where,  $ObjV$  is the objective function, RHT, BWT, and DOPT are the target RH, BW, and RH values, respectively, and  $RH(i)$ ,  $BW(i)$ , and  $DOP(i)$  are the RH, BW, and DOP values, respectively, of the  $i$ th individual. Though the objective function is minimized, the GA tries to maximize the solution. Hence, a proper fitness index is assigned to each solution such that the lower value of the objective function corresponds to the higher fitness values for the solution.



(a)



(b)



(c)

FIGURE 6.—Comparison between the measured and calculated weld-bead shape parameters (a) depth of penetration, (b) reinforcement height, (c) weld-bead width for 316LN stainless steel welds produced by A-TIG welding.

### 3.5. Selection of GA Parameters

As the algorithm's speed of convergence depends on the population size, number of generations, crossover type, crossover rate, and mutation rate, a trial-and-error method was used before arriving at the best combination of the above-mentioned GA parameters. Variations in population size of 50, 100, 200, and 500 in number of generations from 100 to 1000, in crossover rate between 0.55 and to 0.90, and in mutation rate between 0.001 and 0.009 were carried out before optimum values were found. Table 2 lists the GA parameters that produced the best solution for the present problem.

Downloaded By: [Raj, Baldev] At: 07:48 19 June 2007

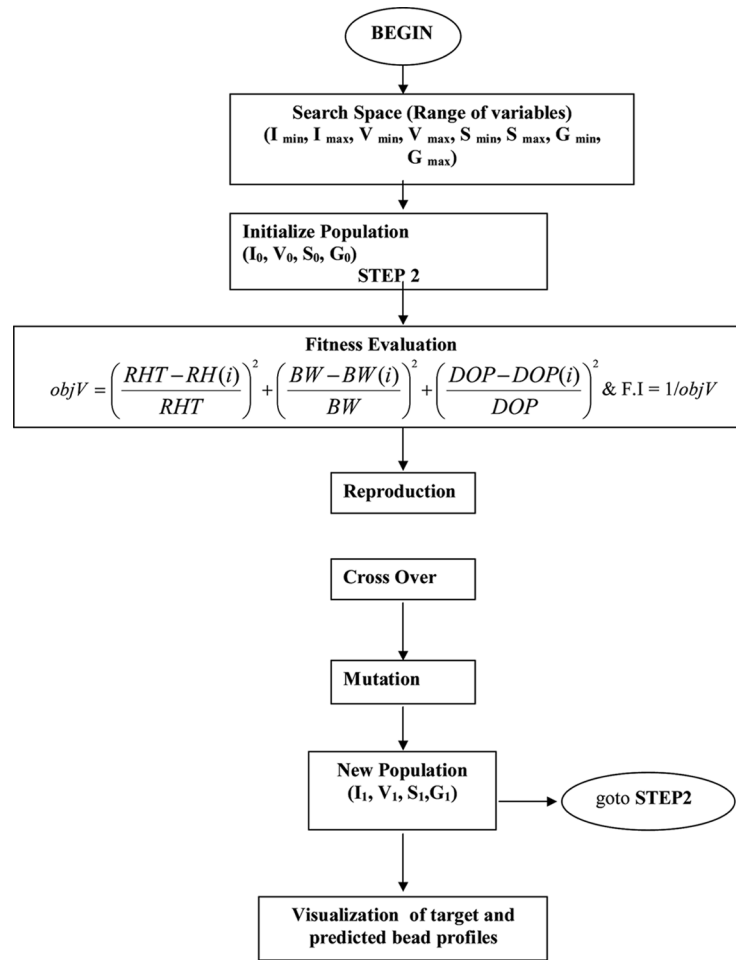


FIGURE 7.—Various steps in genetic algorithm (GA) modeling.

TABLE 2.—Genetic algorithm (GA) parameters selected for optimising the A-TIG welding process.

Genetic algorithm parameters	Value
Population size	50
Number of generations	100
Crossover rate	0.65
Mutation rate	0.005
Type of crossover	Single point

The maximum and minimum values (i.e., the range) for each independent variable  $I$ ,  $V$ ,  $S$ , and  $G$  were also specified. The initial population was selected for the first iteration as specified in the coding, with each individual representing one set of process variables. The members of each individual were encoded in binary format for further processing. The length of each chromosome was taken as the sum of the lengths of each member (gene) of the chromosome in binary format, with the length of 100 individuals being selected as the initial population.

For the present problem, the maximum value among all independent variables was taken as 280 (i.e., the maximum value for  $I$ ), the length of each gene in the

chromosome was taken as 8 ( $2^8 = 256$ ), the number of variables as 4, and the total length of the chromosome as 32 bits ( $4 \times 8$ ). An adequate number of generations of 100 was also specified. All the chromosomes were then evaluated for their fitness using the objective function. All 50 chromosomes were again encoded in binary format (i.e., collection of 0s and 1s) for further reproduction. The encoded chromosomes were ranked based on their value of objective function such that the lower the objective function value the higher the fitness index would be. For selection of the best chromosome among the available 50, the Roulette Wheel Selection (RWS) method was used. In this method, parents are selected according to their fitness. The better the chromosomes are, the more chances to be selected they have. In this method, each individual is assigned a region in a virtual roulette board proportional to its fitness. An unbiased spinning of the roulette pointer is simulated through a random number generator, and the individual corresponding to the region where it points is picked up for further processing often with an assigned probability [13, 27]. Chromosomes with higher fitness will be selected more often. The algorithm selects chromosomes in this fashion until it has generated the entire population of the next generation.



Single Point Crossover (XSOP) was then carried out on the selected chromosome by exchanging the parts on selection position to produce offspring. Minimum error in the predicted weld-bead profile was obtained with the crossover rate of 0.65, implying that crossover was carried out on only 65 percent of chromosomes among the 50 selected chromosomes, and the remaining chromosomes were carried forward to the next operation without any alteration. After crossover, mutation was carried out on the offspring, with the mutation probability kept at a low value of 0.005 to avoid any possible perturbation.

The offspring were then decoded to check their fitness by substituting in the objective function equation, and the offspring are again ranked based on their fitness index. Selection of the next 50 chromosomes was then carried out by mixing the chromosomes of both the parent and offspring, and selecting the best 50 chromosomes based on their fitness or ranking index. The newly selected 50 chromosomes were reinserted for the next iteration. Such iterations were continued until there was no further change in the value of the optimized variable or until the value of the variable remained saturated over ten consecutive iterations. MATLAB/GRAPHICS programming was used to graphically represent the bead geometry to facilitate comparison between the predicted and target weld-bead geometry.

3.6. Validation of the GA-Based Computational Model

In the present work, to demonstrate the working of the GA-based computational models, a few target weld-bead geometries were randomly chosen from the experimentally generated database, and the GA was used to optimize the A-TIG process. Every time the GA code was run, it produced different sets of process variables that can all produce the same target weld-bead geometry. It was found that target weld geometry was attainable via multiple pathways involving various sets of welding process variables. Therefore, the GA model can be utilized to calculate multiple sets of welding process variables, i.e., various combinations of arc current, voltage, torch speed, and arc gap, with each set capable of producing the same target weld geometry. This is in agreement with the findings of Mishra and Debroy [25] who have reported that the GA

TABLE 3.—Comparison between actual and predicted A-TIG process variables and weld-bead shape parameters for 304LN stainless steel welds.

Weld-bead shape parameters and welding process variables	Case I		Case II	
	Actual	Predicted	Actual	Predicted
Bead width, BW (mm)	6.158	6.137	11.025	11.017
Reinforcement height, RH (mm)	0.326	0.260	0.610	0.620
Depth of penetration, DOP (mm)	3.833	3.872	8.158	8.092
Welding current, <i>I</i> (Amps)	140	136	280	280
Welding voltage, <i>V</i> (Volts)	13.6	15	19.4	20
Welding (torch travel) speed, <i>S</i> (mm/sec)	1.33	1.33	1.33	1.33
Arc gap, <i>W</i> (mm)	1.5	1	0.75	0.75

procedure can calculate multiple sets of welding variables, each leading to the same weld geometry. This capability makes the GA superior to regression models and artificial neural networks which can provide only a single set of process variables. Table 3 compares two such cases of target weld-bead geometry with the predicted weld-bead geometry for 304LN stainless steel and the corresponding welding process variables. There was good agreement between the two sets of values. Graphical comparison between the predicted and target weld-bead geometry for case I and case II as listed in Table 3 shown in Fig. 8 clearly proved that predicted weld-bead geometry almost exactly matches target weld-bead geometry. The weld-bead geometry has been generated graphically here by drawing two half-ellipses to get the bead shape. Actual weld cross-sections for the above two cases are shown in Fig. 9. Table 4 compares two cases of target weld-bead geometry with the predicted weld-bead geometry for 316LN stainless steel and the corresponding process variables. There was good agreement between the two sets of values. The graphical comparison between the target and predicted weld-bead geometry shown in Fig. 10 for case I and case II as listed in Table 4 for 316LN stainless steel weld proved that predicted weld-bead geometry almost exactly matches target weld-bead geometry. Actual weld cross-sections of the above two cases are shown in Fig. 11. The shapes of the actual weld geometry do not conform to those of the predicted bead geometry, mainly because regression analysis used in the present model cannot describe the mechanisms taking place in the weld pool which decide the actual shape of

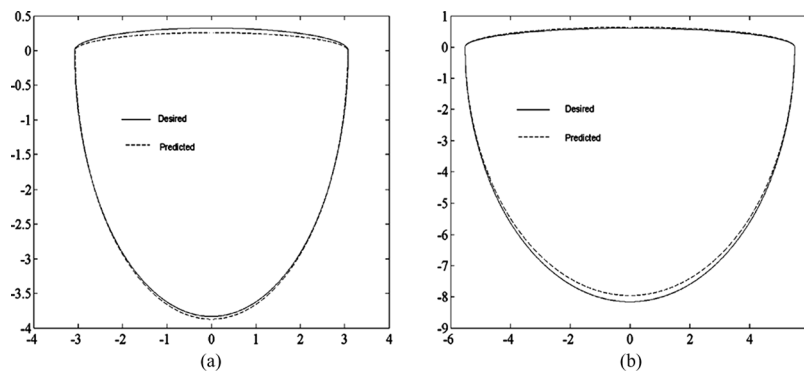


FIGURE 8.—Graphical comparison between the desired and predicted weld-bead geometry using GA optimized process parameters for 304LN stainless steel weld produced by A-TIG welding (a) Case I (b) Case II.

Downloaded By: [Raj, Baldev] At: 07:48 19 June 2007

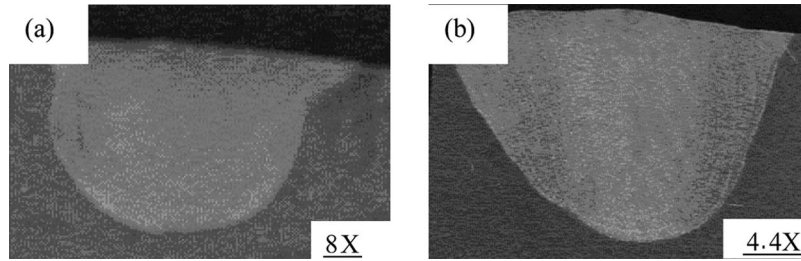


FIGURE 9.—Actual cross sections of the 304LN stainless steel weld produced by A-TIG welding (a) Case I (b) Case II.

TABLE 4.—Comparison between actual and predicted A-TIG process variables and weld-bead shape parameters for 316LN stainless steel welds.

Weld-bead shape parameters and welding process variables	Case I		Case II	
	Actual	Predicted	Actual	Predicted
Bead width, BW (mm)	9.939	9.946	8.828	8.834
Reinforcement height, RH (mm)	0.825	0.803	0.721	0.722
Depth of penetration, DOP (mm)	7.0	7.02	8.136	8.138
Welding current, <i>I</i> (Amps)	280	280	240	246
Welding voltage, <i>V</i> (Volts)	19.8	17	17.3	14
Welding (torch travel) speed, <i>S</i> (mm/sec)	2	1.83	1	1
Arc gap, <i>W</i> (mm)	1.5	1	1.5	0.75

the weld geometry. This is the limitation of the present model. However, it is possible to predict the weld geometry corresponding to actual weld cross-sections by developing phenomenological heat and fluid flow models to calculate the bead geometry [25].

4. CONCLUSIONS

- GA-based computational models have been developed to optimize the A-TIG process parameters to achieve the target weld-bead geometry for welding 304LN and 316LN stainless steels. In this methodology, first regression models correlating weld-bead shape parameters, viz. bead width, depth of penetration, and reinforcement height, with A-TIG process parameters, viz. current, voltage, welding speed, and arc gap, have been developed independently for 304LN and 316LN stainless steels. Good correlation was obtained between the measured and calculated weld-bead shape parameters using the regression models.
- A GA code was developed in which objective function was evaluated using the regression models. The objective function in GA was defined as the sum of least-square error estimates of the weld-bead shape parameters, viz.

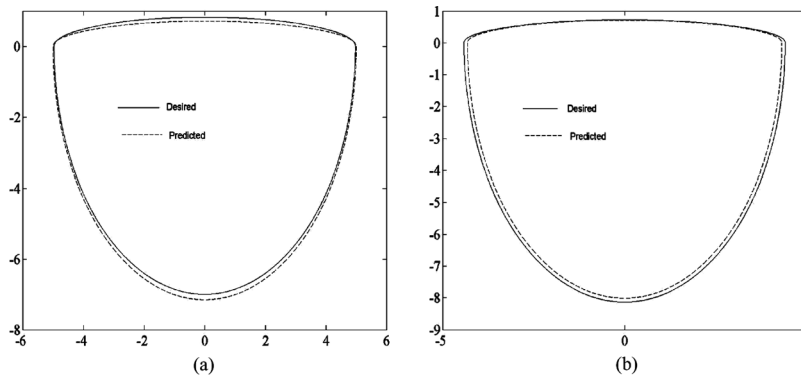


FIGURE 10.—Graphical comparison between the desired and predicted weld-bead geometry using GA optimized process parameters for 316LN stainless steel weld produced by A-TIG welding (a) Case I (b) Case II.

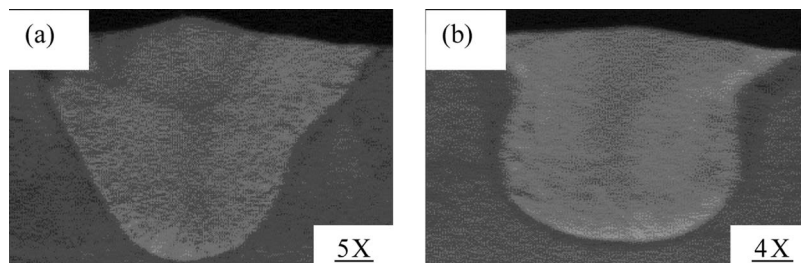


FIGURE 11.—Actual cross-sections of the 316LN stainless steel weld produced by A-TIG welding (a) Case I (b) Case II.

Downloaded By: [Raj, Baldev] At: 07:48 19 June 2007

- depth of penetration, bead width, and reinforcement height.
- To minimize the error in the predicted weld-bead geometry, the GA parameters such as population size, crossover rate, and mutation probability were optimized by trial and error. Close agreement was achieved between weld-bead geometry obtained using the GA optimized process parameters and the target weld bead geometry.
  - The present work has also shown that GA modeling can determine the alternative paths to achieve the target weld-bead geometry by estimating the various sets of process variables that can all produce a target weld-bead geometry.
  - Thus, a GA has been developed for optimizing the A-TIG process parameters to achieve target weld-bead geometry for 304LN and 316LN stainless steels.

## REFERENCES

1. Heiple, C.R.; Roper, J.R. Mechanism for minor element effect on GTA fusion zone geometry. *Welding Journal* **1982**, *61* (4), 97s–102s.
2. Lambert, J.A. Cast-to-cast variability in stainless steel mechanized GTA welds. *Welding Journal* **1991**, *70* (5), 41–52.
3. Jarvis, B.L.; Ahmed, N.U. Development of keyhole mode gas tungsten arc welding process. *Science and Technology of Welding and Joining* **2000**, *5* (1), 1–7.
4. TWI GSP No. 5663, An evaluation of the A-TIG welding process, January, 1994.
5. Anderson, P.C.J.; Wiktorowicz, R. A-TIG welding – The effect of the shielding gas. *TWI Bulletin* 1995, July/August, 76–77.
6. Anderson, P.C.J.; Wiktorowicz, R. Improving productivity with A-TIG welding. *Welding and Metal Fabrication* **1996**, *64* (3), 108–109.
7. Lucas, W. Activating flux – improving the performance of the TIG process. *Welding and Metal Fabrication* **2000**, *68* (2), 7–10.
8. Paskell, T.; Lundin, C.; Castner, H. GTAW flux increases weld joint penetration. *Welding Journal* **1997**, *76* (4), 57–62.
9. Modenesi, P.J.; Apolinario, E.R.; Pereira, I.M. TIG welding with single-component fluxes. *Journal of Materials Processing Technology* **2000**, *99* (1–3), 260–265.
10. Tanaka, M.; Shimizu, T.; Terasaki, H.; Ushio, M.; Koshi-ishi, F.; Yang, C.L. Effects of activating flux on arc phenomena in gas tungsten arc welding. *Science and Technology of Welding and Joining* **2000**, *5* (6), 397–402.
11. Yushchenko, K.A. A-TIG welding of carbon-manganese and stainless steels. Intl. Conf. on Welding Technology, Paton Institute, Paper 2 Cambridge, 13–14, October, 1993.
12. Deb, K. An introduction to genetic algorithms. *Sadhana* **1999**, *24* (4&5), 293–315.
13. Goldberg, D.E. *Genetic Algorithms in Search, Optimization, and Machine Learning*; Addison Wesley, 1989.
14. Deo, B.; Deb, K.; Jha, S.; Sudhakar, V.; Sridhar, N.V. Optimal operating conditions for the primary end of an integrated steel plant. *ISIJ Int.* **1998**, *38*, 98.
15. Rastogi, R.; Deb, K.; Dev, B.; Bloom, R. Genetic adaptive search model of hot metal desulphurization. *Steel Research* **1994**, *65*, 472.
16. Chakraborti, N.; Gupta, R.S.P.; Tiwari, T.K. Optimisation of continuous casting process using genetic algorithm: Studies of spray and radiation cooling regions. *Ironmaking and Steelmaking* **2003**, *30*, 273.
17. Deb, K.; Reddy, A.R.; Singh, G. Materials and Manufacturing Processes **2003**, *18*, 409.
18. Brezocnik, M.; Balic, J.; Kampus, Z. Modelling of forming efficiency using genetic algorithms. *Journal of Materials Processing Technology* **2001**, *109*, 20.
19. Reardon, B.J. Materials and Manufacturing Processes **2003**, *18*, 493.
20. Kim, D.; Rhee, S. Optimisation of arc welding process parameters using a genetic algorithm. *Welding Journal* **2001**, *80* (7), 184s–189s.
21. Kim, D.; Rhee, S.; Park, H. Modelling and optimisation of GMA welding process by genetic algorithm and response surface methodology. *International Journal of Production Research* **2002**, *40* (7), 1699–1711.
22. Kim, D.; Rhee, S. Optimization of GMA welding process using the dual response approach. *International Journal of Production Research* **2003**, *41* (18), 4505–4515.
23. Cemal Meran. Prediction of the optimized welding parameters for the joined brass plates using genetic algorithm. *Materials and Design* **2006**, *27*, 356–363.
24. Correia, D.S.; Gonclaves, C.V.; Junior, S.C.; Ferraresi, V.A. GMAW welding optimisation using genetic algorithms. *Journal of Brazilian Society of Mechanical Science and Engineering* **2004**, *26* (1), 28–33.
25. Mishra, S.; Debroy, T. A heat transfer and fluid flow model to obtain a specific weld geometry through multiple paths. *Journal of Applied Physics* **2005**, *98*, 044902(1)–044902(10).
26. Kumar, A.; DebRoy, T. Tailoring complex weld geometry through reliable heat transfer and fluid flow calculations and a genetic algorithm. *Metallurgical and Materials Transactions, A* **2005**, *36A* (10), 2725–2735.
27. Chakraborti, N. Genetic algorithms in materials design and processing. *International Material Reviews* **2004**, *49* (3–4), 246–260.